

This article may be downloaded for personal use only. Any other use requires prior permission of the author and AIP Publishing.

The following article appeared in J. Vac. Sci. Technol. B **34** (2016) 061207 and may be found at <http://dx.doi.org/10.1116/1.4967300>

Aluminum-based contacts for use in GaSb-based diode lasers

Thanh-Nam Tran^{a)}, Saroj Kumar Patra, Magnus Breivik, and Bjørn-Ove Fimland^{b)}

Department of Electronics and Telecommunications, Norwegian University of Science and Technology (NTNU), NO-7491 Trondheim, Norway

^{a)}Electronic mail: nam.tran@ntnu.no

^{b)}Electronic mail: bjorn.fimland@iet.ntnu.no

Aluminum-based contacts could be a good alternative to conventional gold-based contacts for a number of GaSb-based devices. In this study, the use of some Al-based contacts in GaSb-based diode lasers was investigated via the measurement of specific contact resistivity and laser output characteristics. The Al-based contacts to p-type GaSb(001) exhibited lower specific contact resistivities than the conventional Au-based contacts, whereas the opposite was the case for contacts to n-type GaSb(001). The good performance of GaSb-based laser diodes using Al-based contacts shows the applicability of this type of contact in GaSb-based devices. The contact between Al only and p-type GaSb(001), however, could suffer from a reliability problem when used in diode lasers, due to interdiffusion, in which case a diffusion barrier should be included.

I. INTRODUCTION

GaSb-based diode lasers are one of the promising monochromatic light sources in the mid-infrared wavelength region of 2-5 μm . High-performance operation of these devices

requires ohmic contacts with ultra-low resistivity to enhance the current injection and to minimize the heat generation in the laser structures in order to minimize Auger recombination. Currently, Au-based contacts are predominantly used. Although aluminum contacts have been widely used in silicon integrated-circuits, it has not been reported in use in GaSb-based lasers. Thanks to excellent properties of aluminum, such as low electrical resistance and good contacting with wire bonds (both Au and Al wires), Al-based contacts are promising as a cheaper alternative for GaSb-based devices.

Ti/Pt/Au ohmic contact to p-type GaSb(001) is widely chosen for a number of antimonide-based devices, including for GaSb-based diode lasers, and is a natural choice of Au-based contact that alternative Al-based contacts should be compared with. The specific contact resistivity of this metallization is typically in the order of $10^{-8} - 10^{-6} \Omega \text{ cm}^2$ ¹⁻³. Since every deposited metal can create an ohmic contact to p-type GaSb(001),^{4,5} Al can be used as single-element metallization system. Milnes et al.⁶ have investigated ohmic contacts to p-type GaSb(001), using Al amongst other metals. The authors showed that p-GaSb(001)/Al contact had a low specific contact resistivity which was comparable to those of Au and Ag contacts, but less stable after being heated for 30 hours at temperatures from 200 °C and above. We believe the latter is due to the diffusion of Al into GaSb, in which case it can be avoided by adding a diffusion barrier. Ti is well-known as the diffusion barrier for the Al contacts to Si,⁷ and thus Ti is our candidate for the diffusion barrier in Al contacts to GaSb. The formation of the intermetallic layer TiAl_3 at annealing temperatures above 300 °C which allows Al to diffuse through⁷ is not expected to be an issue as long as the contact is annealed below 300 °C for a rather short time.

In contrast, the Schottky barrier due to the Fermi-level pinning at the surface near the valence band makes ohmic contacts to n-type GaSb(001) more difficult to obtain⁸⁻¹⁰. Forming ohmic contact to n-type GaSb(001) mostly bases on the formation of intermetallic compound

at the metal – semiconductor interface by the use of multilayer contacts and annealing¹¹. The metals Pd and Ni are widely chosen to make intermetallic compound with n-type GaSb(001),¹²⁻¹⁵ where the primary function is to initiate reactions with GaSb and to serve as an adhesion layer⁵. Ge can be used to create a highly doped n⁺-GaSb layer in order to provide a tunneling contact¹⁶. Our choice of Au-based contact here, that alternative Al-based contacts should be compared with, is a specific Pd/Ge/Au/Pt/Au metal stack contact that has shown excellent performance¹². Although an alternative Ni/Ge/Au/Pt/Au contact has shown even lower specific contact resistivity, we chose Pd over Ni as there is some uncertainty regarding how stable Ni would be as compared to Pd in long term thermal stability¹². Utilizing the advantages of solid phase reaction of the Pd/Ge contact, we propose an Al-based metallization system to n-type GaSb(001) consisting of Pd, Ge, Ti and Al.

In this work, the specific contact resistivities of Al-based contacts to p- and n-type GaSb(001) are measured and compared to those of the selected Au-based contacts. Subsequently, the use of these Al-based contacts in GaSb-based lasers is examined via the laser performance. Furthermore, the reliability of the Al-based contacts for laser applications is evaluated in a laser burn-in and life-time test.

II. EXPERIMENTS

A. *Material growths*

To determine the specific contact resistivity of Al-based contacts, the transfer length method (TLM) and four-probe measurements were performed on samples grown by molecular beam epitaxy (MBE)^{3,17}. For the contacts to p-type GaSb(001), a 2 μm thick epitaxial layer of Be-doped GaSb was grown on a 100 nm thick undoped GaSb buffer layer grown on n-type GaSb(001) wafer (with nominal carrier concentration of $5 \times 10^{17} \text{ cm}^{-3}$) in a solid source Varian GEN II Modular MBE system. The p-type doping concentration was $2 \times$

10^{19} cm^{-3} , which is a typical concentration for the cap layer of the laser structure. For the contacts to n-type GaSb(001), a 2 μm thick epitaxial layer of Te-doped GaSb was grown on semi-insulating GaAs(001) wafer. For the n-type sample, nominal carrier concentration was $5 \times 10^{17} \text{ cm}^{-3}$, which is similar to the carrier concentration of n-type GaSb(001) substrates used for laser growth.

The laser structure, shown schematically in Figure 1, was grown in the above-mentioned MBE system equipped with Veeco valved cracker cells for both arsenic and antimony.

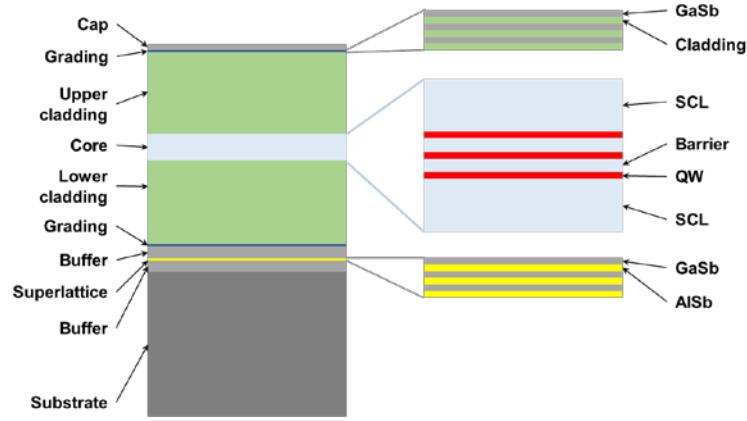


FIG. 1. (Color online) Schematic of the growth structure of the lasers. (Details are given in Section II A.)

The 2 μm thick lower cladding layer of n-type $\text{Al}_{0.9}\text{Ga}_{0.1}\text{As}_{0.06}\text{Sb}_{0.94}$ was doped with Te to a carrier concentration level of $1.6 \times 10^{17} \text{ cm}^{-3}$ for the first 1.6 μm and then the doping level was graded to a carrier concentration level of $1.0 \times 10^{17} \text{ cm}^{-3}$ over the next 400 nm towards the active region of the laser. The 2 μm thick upper cladding layer of p-type $\text{Al}_{0.9}\text{Ga}_{0.1}\text{As}_{0.06}\text{Sb}_{0.94}$ was Be-doped with a grading in carrier concentration from $2.0 \times 10^{17} \text{ cm}^{-3}$ to $5.0 \times 10^{18} \text{ cm}^{-3}$ over the first 400 nm and then constant doping with carrier concentration at $5.0 \times 10^{18} \text{ cm}^{-3}$ for the next 1.6 μm . The grading in carrier concentration was achieved by varying the temperature of dopant sources linearly with time. A 12 nm thick

doped (nominal average carrier concentration of $4.1 \times 10^{17} \text{ cm}^{-3}$) GaSb/AlSb superlattice structure was introduced within the Te-doped GaSb buffer layer on top of the Te-doped GaSb(001) substrate to minimize the propagation of any dislocation defects towards the active region. The nominal carrier concentration in the Te-doped GaSb buffer layer and Te-doped GaSb(001) substrate was $5 \times 10^{17} \text{ cm}^{-3}$. To help carrier injection, heavily doped graded bandgap transition layers were grown between the buffer layer and the n-type cladding layer and between the p-type cladding layer and the heavily doped p-type (Be dopant concentration of $2 \times 10^{19} \text{ cm}^{-3}$) GaSb cap layer. The active region of the laser consisted of three 12 nm wide $\text{In}_{0.33}\text{Ga}_{0.67}\text{As}_{0.1}\text{Sb}_{0.9}$ quantum wells (QW) separated by 20 nm wide $\text{Al}_{0.35}\text{Ga}_{0.65}\text{As}_{0.026}\text{Sb}_{0.974}$ barriers and sandwiched between two 145 nm wide undoped $\text{Al}_{0.35}\text{Ga}_{0.65}\text{As}_{0.026}\text{Sb}_{0.974}$ separate confinement layers (SCL).

B. Device fabrications

TLM structures were defined by conventional UV-lithography and were isolated on rectangular mesas by Inductively-Coupled Plasma – Reactive Ion Etching (ICP-RIE)³. The metallization was performed by e-beam evaporation in a combined sputtering and e-beam evaporation system (AJA ATC-2200V) at a starting pressure of 10^{-7} Torr. The contact formation is summarized in Table I. Prior to metallization, *in situ* cleaning of the GaSb surface by low-ion-energy (325 eV) Ar^+ irradiation was applied to remove the native oxide³. After lift-off, the samples underwent a rapid thermal anneal at 290 °C for 45 s in nitrogen atmosphere, which is an optimized annealing procedure¹² for the n-type GaSb/Pd/Ge/Au/Pt/Au contact that we use as a comparison reference for the performance of Al-based contacts to n-type GaSb. For GaSb-based diode lasers, the optimized annealing procedure for contacts to n-type GaSb is simultaneously also applied for the Ti/Pt/Au contacts to p-type GaSb during laser fabrication. As our Al-based contacts to n-type GaSb also include

Pd/Ge, we thus use the same annealing procedure for all annealed contacts. Samples of non-annealed Al contact to p-type GaSb(001) were also prepared to investigate the effect of Al diffusion on the contact properties.

Ridge-waveguide lasers using Al-based and Au-based contacts with 25 μm wide strips, as shown in Figure 2, were processed using ICP-RIE (Oxford Plasma System 100 ICP380 reactor) with BCl_3/Cl_2 chemistry. The etch stop was controlled precisely, as described in detail in ref. 18, to 100 nm above the active region, using *in situ* reflectance monitoring. For mesa passivation, photoresist ma-N440 was spin-coated followed by thermal hardening and RIE etchback with O_2/CF_4 chemistry. The metallization of the laser contacts presented in Figure 2 and Table II were performed as in the specific contact resistivity experiments, except using an optimized Ar ion energy of 180 eV to remove GaSb native oxide³. To achieve good bonding to the aluminum contact, 50 nm of SiO_2 was added to improve the adhesion between photoresist and Al. In addition, a thick layer of Al is required to reduce the bonding force. We observed non-lasing behavior of the laser when the bonding force exceeded 80 grams. After top contact metallization, the laser samples were thinned down to about 150 μm before applying the bottom contact metallization. Finally, all lasers were annealed following the mentioned annealing procedure and were cleaved into 1.5 mm long laser bars before being mounted episcide-up on copper heat sinks. No facet coating was applied. The laser diodes were characterized in continuous wave operation at 16 °C, lasing at 2.29 μm wavelength. The reliability of the Al-based contacts was examined in a laser burn-in and life-time test. The test conditions are summarized in Table II. Laser properties such as output power and I-V characteristic were recorded to evaluate the contact reliability.

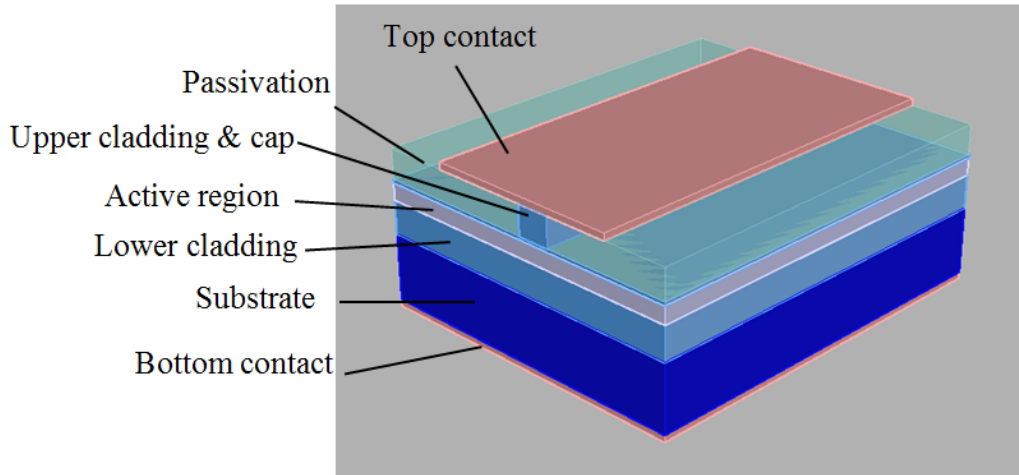


FIG. 2. (Color online) 25 μm wide ridge waveguide laser using different types of contacts. **Laser A:** Al top contact and Pd/Ge/Ti/Al bottom contact. **Laser TA:** Ti/Al top contact and Pd/Ge/Ti/Al bottom contact. **Laser TPA:** Ti/Pt/Au top contact and Pd/Ge/Au/Pt/Au bottom contact.

III. RESULTS AND DISCUSSIONS

The Al-based contacts to both p- and n-type GaSb(001) exhibited low specific contact resistivity and comparable to the Au-based contacts. The results are summarized in Table I.

Similar to Ti⁵, Al can react with p-type GaSb, even at room temperature¹⁹, to provide good ohmic contact. However, unlike the contact between Ti and p-type GaSb(001), where the contact resistivity is not affected by annealing¹⁴, the interdiffusion between Al and p-type GaSb(001) during annealing improves the contact resistivity. After annealing, the measured value of ρ_c for the Al contact to p-type GaSb(001) is lower than both for the as-deposited Al contact and for the Au-based contact. It is one of the lowest reported results for contact to p-type GaSb(001). However, it is also quite a bit below the lower limit ($5 \times 10^{-8} \Omega \text{ cm}^2$ in this case³) for accurate/valid results of the measurement method, and thus there is a relatively high

uncertainty attached to this value. This is supported by the fact that the measurements of two out of three annealed Al samples gave negative contact resistances (R_c) with small absolute values similar to the positive contact resistance of the third sample, indicating that the TLM failed to determine accurately the extremely low specific contact resistivity of the Al contact to p-type GaSb after annealing. The metal contact to p-type GaSb(001) consisting of Ti and Al also exhibited a very low specific contact resistivity which is unexpectedly lower than that of the Au-based contact, even though Ti is the first deposited metal in both cases.

TABLE I. Contact preparation and the measured specific contact resistivity for each metallization.

Contact	Metallization	N	Thickness (Å)	Average ρ_c ($\Omega \text{ cm}^2$)
p-type GaSb	Non-annealed Al	3	2000	7.8e-8 (for N=3)
	Annealed Al	3	2000	1.4e-8 (for N=1*)
	Ti/Al	3	500/2000	2.0e-8 (for N=3)
	Ti/Pt/Au	5	500/250/3250	10.5e-8 (for N=5)
n-type GaSb	Pd/Ge/Al	3	87/560/2000	3.3e-3 (for N=3)
	Pd/Ge/Ti/Al	3	87/560/500/2000	2.6e-3 (for N=3)
	Pd/Ge/Au/Pt/Au	3	87/560/233/476/2000	1.2e-3 (for N=3)

N: number of samples

* Measurement results of the other two samples gave negative contact resistances with small absolute values similar to the positive contact resistance (R_c), and thus there is a relatively high uncertainty attached to the listed value.

For the contacts to n-type GaSb(001), an ohmic behavior was observed from I-V curves in all samples. The Au-based contact showed the lowest average ρ_c while the Al-based contact using Ti as a diffusion barrier showed a slightly lower average ρ_c than the Al-based contact without Ti. The observed high value of ρ_c for both Au-based and Al-based contacts is

likely due to the low doping level (i.e. carrier concentration) of the n-type GaSb epi-layer. Consequently, the value of ρ_c would improve if the carrier concentration in the n-GaSb epi-layer was increased. This, however, is not applicable for the case of GaSb-based lasers as fabricated in this study as high quality n-type GaSb(001) wafers with much higher carrier concentration (e.g. above $2 \times 10^{18} \text{ cm}^{-3}$) are in general not commercially available.

Representative output power and current-voltage characteristics of as-fabricated lasers are shown in Figure 3. All lasers exhibit similar performance. Compared to the lasers with Au-based contacts (Laser TPA), the lasers with Al-based contacts (Laser A and Laser TA) had higher resistance, most likely due to the bottom contact.

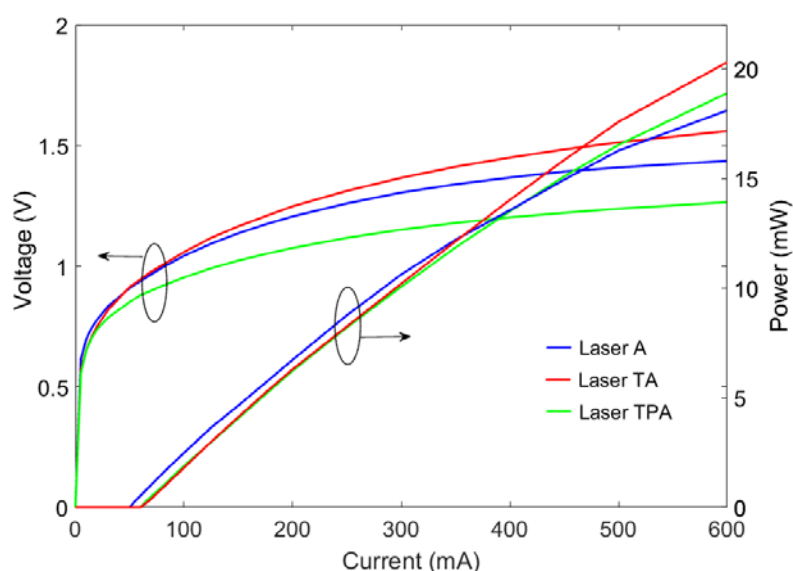


FIG. 3. (Color online) Representative output power and current-voltage characteristics of as-fabricated lasers. (Laser A: Al top contact, Laser TA: Ti/Al top contact, Laser TPA: Ti/Pt/Au top contact.)

After the burn-in test, no degradation, as judged by output power, was observed from any of the lasers. Some lasers with Laser A contacts had even higher output power than as-fabricated devices. After the life-time test, the output power of lasers with Laser A contacts

degraded ca. 5-15%, whereas the lasers with Laser TA or Laser TPA contacts showed no degradation. The degradation in output power of the lasers with Laser A contacts was attributed to an increase in the total resistance of the laser, see Figure 4, probably due to Al diffusion during burn-in causing a degradation of the top contact. We believe the Ti in the Laser TA top contact reduces the Al diffusion during the life-time test, and thus prevents degradation of the lasers with Laser TA contacts. Finally, we note that using the TiAl top contact in combination with the conventional PdGeAuPtAu bottom contact should potentially give an even better laser diode performance than demonstrated here.

TABLE II. Reliability test for GaSb-based laser diodes using different types of contacts.

Test	Type of laser	Contacts (Top/Bottom)	Number of samples	Time (h)	Current density (A/cm ²)	Output power after testing
1 st –	Laser A	Al/PdGeTiAl	5	100	800	No degradation
Burn-in	Laser TA	TiAl/PdGeTiAl	4	100	800	No degradation
(16 °C)	Laser TPA	TiPtAu/PdGeAuPtAu	3	100	800	No degradation
2 nd –	Laser A	Al/PdGeTiAl	5	100	1200	5-15% degradation
Life-time	Laser TA	TiAl/PdGeTiAl	4	100	1200	No degradation
(80 °C)	Laser TPA	TiPtAu/PdGeAuPtAu	3	100	1200	No degradation

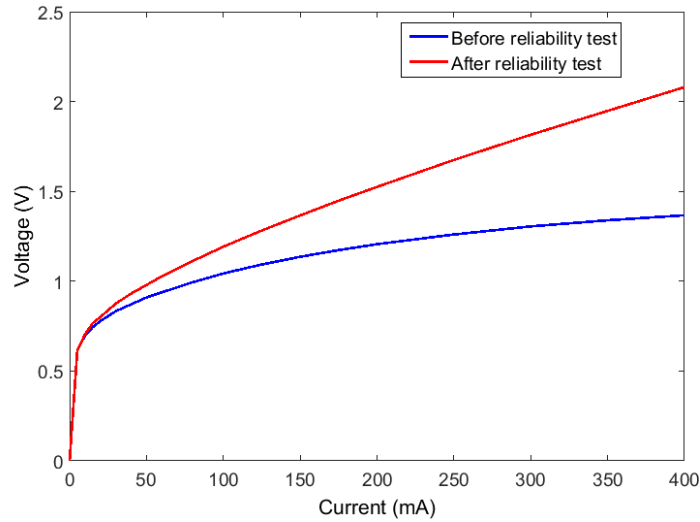


FIG. 4. (Color online) Typical I-V characteristic of lasers with Laser A contacts before and after reliability test.

IV. CONCLUSIONS

We found that the Al-based contacts to p-type GaSb(001) exhibited around five times lower specific contact resistivities than the conventional Au-based contacts, whereas the opposite (two-three times higher) was the case for contacts to n-type GaSb(001). However, as revealed by our reliability test, the contact between Al only and p-type GaSb(001) could suffer from a reliability problem when used in some devices, due to interdiffusion, in which case a diffusion barrier should be included. The GaSb-based laser diodes with TiAl/PdGeTiAl top/bottom contacts proved to have equally good performance, in terms of power output and reliability, as the laser diodes with conventional TiPtAu/PdGeAuPtAu top/bottom contacts, which is promising with regard to the applicability of Al-based contacts in GaSb-based devices.

ACKNOWLEDGMENTS

The authors would like to acknowledge the Norwegian University of Science and Technology (NTNU) for support (from the Strategic Area Materials program) and the Research Council of Norway for the support to this work (Grant 177610/V30) and to the Norwegian Micro- and Nano-Fabrication Facility, NorFab (Grant 197411/V30).

¹B. Tadayon, C. S. Kyono, M. Fatemi, S. Tadayon, and J. A. Mittereder, *J. Vac. Sci. Technol. B* **13**, 1 (1995).

²F. Y. Soldatenkov, S. V. Sorokina, N. K. Timoshina, V. P. Khvostikov, Y. M. Zadiranov, M. G. Rastegaeva, and A. A. Usikova, *Semiconductors* **45**, 1219 (2011).

³N. T. Tran, S. K. Patra, M. Breivik, and B.-O. Fimland, *J. Vac. Sci. Technol. B* **33**, 061210 (2015).

⁴J. O. McCaldin, T. C. McGill, and C. A. Mead, *J. Vac. Sci. Technol.* **13**, 802 (1976).

⁵A. Vogt, A. Simon, J. Weber, H. L. Hartnagel, J. Schikora, V. Buschmann, and H. Fuess, *Mater. Sci. Eng. B* **66**, 199 (1999).

⁶A.G. Milnes, M. Ye, and M. Stam, *Solid State Electron.* **37**, 37 (1994).

⁷M. Lawrence, and A. Dass, *Characterization in Silicon Processing*, edited by Y. Strausser (Butterworth-Heinemann, Boston, 1993).

⁸W. E. Spicer, I. Lindau, P. Skeath, C. Y. Su, and P. Chye, *Phys. Rev. Lett.* **44**, 420 (1980).

⁹Z. M. Lü, D. Mao, L. Soonckindt, and A. Kahn, *J. Vac. Sci. Technol. A* **8**, 1988 (1990).

¹⁰K. M. Schirm, P. Soukiassian, P.S. Mangat, and L. Soonckindt, *Phys. Rev. B* **49**, 5490 (1994).

¹¹D. G. Ivey, *Platin. Met. Rev.* **43**, 2 (1999).

- ¹²N. Rahimi, A. A. Aragon, O. S. Romero, D. M. Kim, N. B. J. Traynor, T. J. Rotter, G. Balakrishnan, S. D. Mukherjee, and L. F. Lester, Proc. SPIE **8620**, 86201K (2013).
- ¹³W. S. Tse, R. H. Chen, C. S. A. Fang, and J. R. Chen, Appl. Phys. A **54**, 556 (1992).
- ¹⁴A. Vogt, H. L. Hartnagel, G. Miehe, H. Fuess, and J. Schmitz, J. Vac. Sci. Technol. B, **14**, 3514 (1996).
- ¹⁵J. A. Robinson, and S. E. Mohny, J. Appl. Phys. **98**, 033703 (2005).
- ¹⁶A. Vogt, A. Simon, H. L. Hartnagel, J. Schikora, V. Buschmann, M. Rodewald, H. Fuess, S. Fascko, C. Koerdt, and H. Kurz, J. Appl. Phys. **83**, 7715 (1998).
- ¹⁷D. K. Schroder, *Semiconductor Material and Device Characterization* (Wiley-IEEE Press, New Jersey, 2006).
- ¹⁸N. T. Tran, M. Breivik, S. K. Patra, and B.-O. Fimland, Proc. SPIE **9134**, 91342E (2014).
- ¹⁹W. Oueini, M. Rouanet, and J. Bonnet, Surf. Sci. **409**, 445 (1998).